J Appl Electrochem (2009) 39:2409–2414
DOI 10.1007/s10800-009-9928-9

ORIGINAL PAPER

Electro-reduction of oxygen and electro-oxidation of methanol at Pd monolayer-modified macroporous Pt electrode

Yongling Du · Kangle Lv · Biquan Su · Nuo Zhang · Chunming Wang

Received: 11 December 2008 / Accepted: 6 May 2009 / Published online: 19 June 2009

Abstract With polystyrene latex spheres self-assembled on indium tin oxide-coated glass electrode as templates, highly ordered macroporous Pt was prepared by electrochemical deposition. Then, the macroporous Pt was modified by Pd monolayer involving the galvanic displacement of Cu monolayer formed by under-potential deposition on macroporous Pt. Electrocatalytic properties of the Pd-modified macroporous Pt electrode for oxygen reduction were investigated by cyclic voltammetry and chronoamperometry in O_2-saturated solution containing 0.1 M $HClO_4$. Methanol electro-oxidation on the Pd-modified macroporous Pt surfaces in 0.5 M H_2SO_4 containing 1 M CH_3OH was studied by cyclic voltammetry. The corresponding results showed that Pd-modified macroporous Pt electrode had negative catalytic activity for methanol oxidation in compared with macroporous Pt. However, Pd-modified macroporous Pt electrode had positive electrocatalytic activity to O_2 reduction.

Keywords Macroporous Pt · Pd monolayer · Oxygen reduction · Methanol oxidation

1 Introduction

Electrocatalytic oxygen reduction (ORR) has become the focus of considerable attention due of its slow kinetics and the need for better electrocatalysts for fuel cell cathodes in the recent years [1, 2]. The central point is that the reduction of oxygen to water is a very slow reaction particularly in acid solution. The high OH coverage on Pt has been shown to inhibit ORR [3]. One of the ways for solving the problem is by developing binary catalysts doped by another transition metal (M, where M = Pd, Co, Cu, V, Fe or Ni) [3–8], which improves the catalytic activity and stability related to those pure metals. In order to increase the efficiency, the catalysts used in practice are usually in the form of nanoparticles. Three types of catalytic nanoparticles are of recent interest: (1) nanoparticles supported on metals, nanotubes, or polymers [9–11] (2) nanoparticles encapsulated in dentrimers [12] and (3) three dimensional (3D) nanoparticles with highly ordered structure [13]. Among them, porous transition metals are of great significance in chemical catalysis. Self-assembled colloidal crystals stand out as ideal templates for creating highly ordered 3D structures with interconnected macropores, which show potential applications related to fuel cells, such as methanol oxidation and O_2 reduction [13, 14].

Direct methanol fuel cells (DMFCs) are considered to be one of the most promising options for addressing future energy needs. DMFCs provide a clean and mobile power source with high-energy conversion efficiency and low pollutant emissions [15]. Platinum is considered one of the most efficient materials for the oxidation of methanol. However, it is susceptible to poisoning effects, due to strongly adsorbing intermediates, such as CO, which are formed during the electrode process [16, 17]. The alloying of a second or even third metal component to platinum has been the favored method for producing CO-tolerant anode catalysts [18–20]. According to bi-functional mechanism, the second metal provides an oxygenated surface species by dissociating water at the second metal sites at lower potential against pure Pt sites, leading to the accelerated CO_2 formation and a decrease in the CO poisoning, thus improving the CO tolerance [21].

Y. Du · K. Lv · B. Su · N. Zhang · C. Wang (✉)
Department of Chemistry, Lanzhou University, Tianshui Road 222, 730000 Lanzhou, People's Republic of China
e-mail: wangcm@lzu.edu.cn

In recent years, new methods for designing electrocatalysts at the atomic level are gaining more and more attention [22]. The modification methods involve underpotential deposition (UPD) [23], spontaneous deposition [24], and other complex methods, such as electron beam lithography [25]. A monolayer can be deposited following a new process involving the galvanic displacement of a monolayer of a non-noble metal by a monolayer of a more noble metal [26].

In this article, we describe the use of electrochemical deposition through an artificial opal template made from polystyrene spheres assembled on ITO electrode surface to produce thin macroporous films of polycrystalline platinum containing highly ordered regular three-dimensional arrays of interconnected spherical macro voids arranged in a closely packed structure. Then, the electrode was immersed in toluene to dissolve the polystyrene and leave the platinum macroporous film. The Pd monolayer was deposited on Pt inverse opal through the displacement of copper monolayer.

2 Experimental

2.1 Chemicals and instruments

All chemicals employed were of analytical reagents grade, and were prepared with deionised water purified via Milli-Q unit. The working electrode (1.0 × 1.0 cm) was an indium-tin oxide (ITO)-coated glass. Prior to use, ITO electrode was cleaned by an ultrasonic cleaner for 15 min in acetone, 15 min in ethanol, and 15 min in deionised water, and then, the ITO was dried by pure nitrogen gas.

The surface morphology of the macroporous Pt attached on ITO surface was characterized with scanning electron microscopy (JSM-6701 F Japan). The crystalline structure of the deposition was identified by XRD (Rigaku D/max-2400, Cu Kα radiation, $\lambda = 0.1541$ nm). X-ray photoelectron spectroscopy (XPS) was performed on a VG Escalab 210 electron spectrometer equipped with Al Kα X-ray radiations ($hv = 1486.6$ eV) as the source for excitation. The binding energy of the C1 s of graphite (284.80 eV) was taken as reference. Electrochemical measurements were performed with CHI660A electrochemical workstation (USA). An IRIS Advantage ER/S inductively coupled plasma emission spectrometer, Thermo Jarrel Ash (Franklin, MA, USA), was used for Platinum determination. The mass loading of catalyst (mg cm^{-2}) was measured by ICP. Pt catalyst was electrodeposited on the PS template which was immersed into toluene to remove the template, and then, the catalyst was dissolved in aqua fortis for detection by ICP with a resolution of 0.01 μg mg^{-1}. Platinum wire was used as counter electrode, and Ag/AgCl (3 M KCl) was the reference electrode. Unless otherwise stated, all the measurements were performed in solutions purged with high pure nitrogen and at room temperature.

2.2 Preparation of template

A colloidal solution of monodispersed polystyrene (PS) spheres with a diameter of 360 nm was synthesized by an emulsifier-free emulsion polymerization technique [27]. A conventional vertical deposition method [28] was used to assemble the PS spheres on the ITO substrate into a face-centered cubic (fcc) close pack. A drop of monodisperse PS solution (1.5%) was placed onto ITO glass and allowed to evaporate to dry at room temperature. Then, the PS layer was heated in a vacuum at 70°C for 30 min to flatten the PS contacts into ITO area.

2.3 Fabrication of macroporous Pt and Pd-modified macroporous Pt

PS-opal/ITO substrates were used as the substrate electrodes for macroporous Pt electrode. Platinum was electrodeposited into the interstitial space of the opal matrix by pulse deposition in 0.1 M $HClO_4$ containing 0.2 mM Hexachloroplatinic acid and 1.0 mM copper ions. Copper ion acts as the surfactant to enhance platinum deposition, just in our former study [29]. A Pd monolayer was deposited on macroporous Pt by the galvanic displacement of a Cu monolayer obtained by under-potential deposition (UPD).

3 Results and discussions

3.1 The characteristic of macroporous Pt electrode and Pd-modified macroporous Pt electrode

Figure 1a shows a typical SEM image of the PS macrospheres synthesized by the surfactant-free emulsion polymerization. The average particle size is around 360 nm. With the vertical deposition method under proper conditions, highly ordered PS colloidal crystals can be formed on the ITO substrate. Figure 1b shows an SEM image of macroporous Pt electrode, whose template has been dissolved in toluene. The macroporous materials of Pt reveal an ordered arrangement of void, which are the exact inverse replica of PS opal. There are some cracks in the macroporous Pt, which result in non-uniform deposition in the crystal and lead to the formation of defects in the replica.

In order to determine the crystalline structure of the catalyst, X-ray diffraction was used. The XRD pattern of

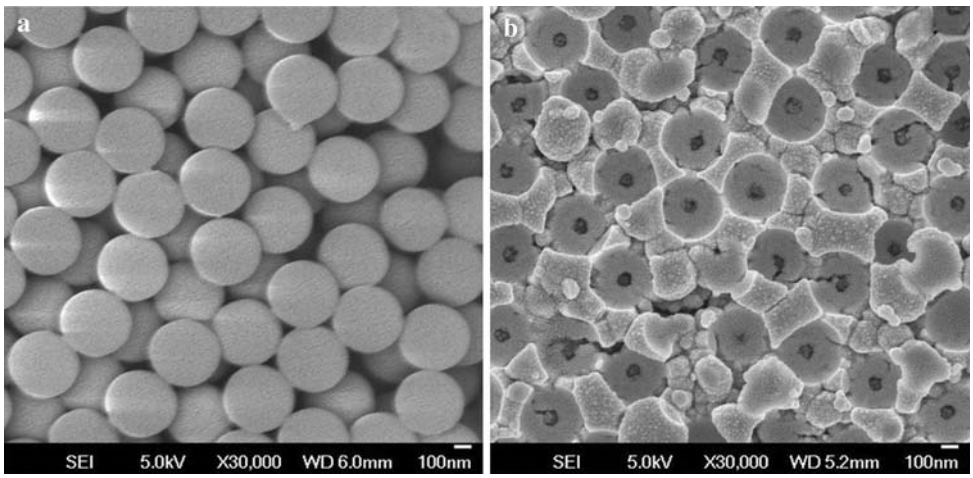

Fig. 1 SEM images of PS macrospheres and macroporous Pt/ITO: **a** PS and **b** macro-porous Pt/ITO

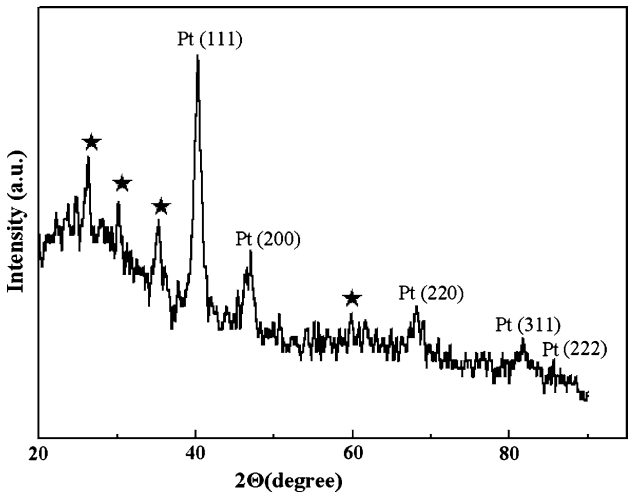

Fig. 2 XRD diffraction pattern of the macroporous Pt. ★ Peaks from the ITO glass substance

the ITO and a catalyst (macro-porous Pt) are shown in Fig. 2. Peaks consistent with the face-centered cubic (fcc) expected for Pt are clearly observed, whereas those marked with ★ are assigned to the ITO glass substrate. XPS measurement was also performed to identify and characterize the copper UPD-modified Pt inverse opal and Pd monolayer-modified Pt inverse opal as shown in Fig. 3. Two XPS bands appeared at 71.3 eV and 74.6 eV, corresponding to the Pt $4f_{7/2}$ and Pt $4f_{5/2}$ signal, respectively, which demonstrated the formation of Pt(0) state (Fig. 3a). The main Cu $2p_{3/2}$ peak, located at 934.2 eV in Fig. 3b, is associated to metallic copper, which confirms that copper successfully deposits on macroporous Pt electrode, whereas Cu^{2+} has one main peak at 933.5 eV (peak 2) and shake up satellites (peaks 3 and 4) at higher binding energies. The relative intensities of the satellites from these levels are indicative of the presence of Cu^{2+} at the surface that refers to a sample which is partially oxidized and little Cu^{2+} residual. Figure 3c displays XPS Pd 3d spectra for Pd films deposited through displacement on macroporous Pt electrode. The Pd 3d spectra locate at 335.7 eV and 341.0 eV, which corresponds to metallic palladium. Weak peaks located at 338.1 eV and 343.2 eV can be contributed to Pd^{2+} which means that there is little Pd^{2+} residual on macroporous Pt electrode.

3.2 Copper under-potential deposition on macroporous Pt electrode

The cyclic voltammogram (CV) (5 mV s^{-1}) of macroporous Pt electrode in 0.1 M $HClO_4$ aqueous solution containing 1.0 mM $CuSO_4$ and 0.30 mM Cl^- is shown in

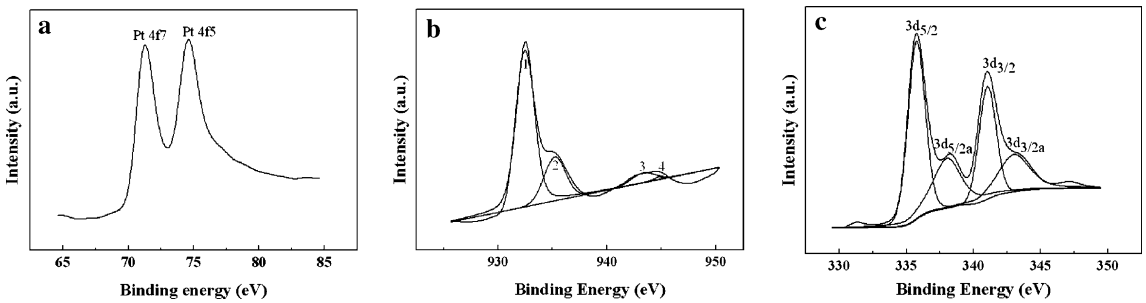

Fig. 3 **a** The Pt 4f XPS of macro-porous; **b** XPS spectra of Cu 3p region of Cu UPD on macroporous Pt; **c** The XPS spectra of the Pd 3d region of Pd-modified macro-porous Pt

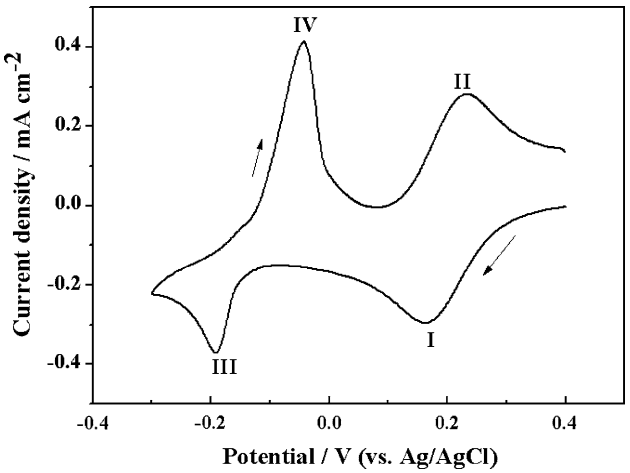

Fig. 4 Cyclic Voltammograms of macro-porous Pt electrode in N_2-saturated solution. Containing 1.0 mM $CuSO_4$ and 0.1 mM Cl^-, scan rate 5 mV s^{-1}

Fig. 4. Two cathodic peaks (I and III) can be observed at about +0.162 V and −0.192 V on the forward scanning. The peak at +0.162 V (peak I) is consistent with the formation of UPD copper on macroporous Pt electrode. The peak at −0.1 92 V (peak III) refers to bulk copper deposition. Two anodic peaks (II and IV) are obtained on the positive scanning, corresponding to the stripping of bulk and UPD copper, respectively. Under-potential deposition, which involves a monolayer-limited process at potentials above the thermodynamic values, was used to coat macroporous Pt surface with a monolayer of Cu. Under-potential deposition occurs at potentials more positive than the equilibrium potential of the deposition reaction [30]. Such a process is energetically unfavorable, and it can occur only due to a strong interaction between the two metals, with their interaction energies changing the overall energetics to favorable. Consequently, only one monolayer can be deposited, and this is a very convenient way to produce well-controlled monolayer. In this study, Cu deposition was carried out by constant potential (0.05 V) which was more positive than the potential of bulk deposition (−0.192 V). The deposited potential is selected to ensure that copper deposition on macroporous Pt at the potential is monolayer.

3.3 Pd monolayer deposition

The electrocatalysts were prepared by a new method for depositing Pd monolayer involving the galvanic displacement by Pd of an under-potentially deposited (UPD) Cu monolayer on the macroporous Pt electrode. After the deposition of Cu from 1.0 mM $CuSO_4$ and 0.30 mM Cl^- in 0.10 M $HClO_4$ solution, the macroporous Pt electrode covered with this Cu monolayer was rinsed to remove Cu^{2+} from the film and placed into a 1.0 mM $PdCl_2$ containing 0.50 M H_2SO_4 solution in an N_2 atmosphere. After a 10-min immersion, the copper monolayer was completely replaced by Pd, which can be summarized as the follow reaction:

$$Pd^{2+} + Cu(upd) = Pd^0 + Cu^{2+} \quad (1)$$

3.4 Oxygen reduction on Pd modified macroporous Pt electrode and macroporous Pt electrode

Figure 5 shows the CVs obtained for the reduction of O_2 with the macroporous Pt electrode and Pd-modified macroporous Pt electrodes in O_2-saturated 0.1 M $HClO_4$ solution. In order to assess the influence of the monolayer Pd coating on the macroporous Pt electrode behavior, the electrocatalytic oxygen reduction of the system was examined. Oxygen reduction begins at 0.50 V and the reduction peak centered at 0.38 V for the Pd-modified macroporous Pt, while small reduction current appears for corresponding macroporous Pt electrode from +0.60 to 0.45 V. The reduction potential is more positive than those reported for oxygen reduction on Pt nanoparticles films [14] and Dendrimer-encapsulated Pt nano-particles [31]. The results provide clear evidence that Pd-modified macroporous Pt electrodes have good electrocatalytic activity for oxygen reduction. The very high catalytic activity measured for the Pd-modified macroporous Pt, with Pd adsorbing OH or O_2 strongly, reflects the decreased OH

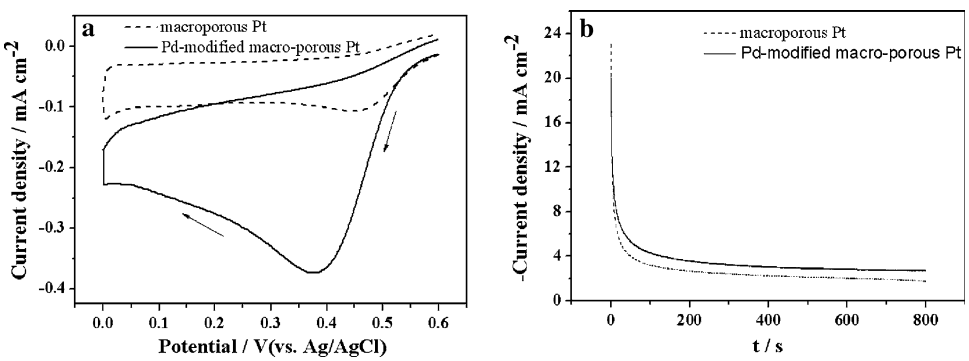

Fig. 5 **a** Cyclic voltammograms at Pd-modified macroporous Pt electrode and macroporous Pt electrode in O_2-satuated 0.1 M $HClO_4$, scan rate 10 mV s^{-1}; **b** CA imagine of Pd-modified macro-porous Pt (*solid line*) and macro-porous Pt (*dashed*) in O_2 saturated 0.1 M $HClO_4$ at constant potential 0.40 V

coverage on Pt [32], thereby enhancing the ORR. The mass loading of catalyst is 0.087 mg cm^{-2}, which was determined by ICP. The mass loading of macroporous Pt electrode was less than that reported by Liu, but the mass activity was more active than that reported by him [33]. The technique is grateful to design catalysts for practical applications since it can enhance the activity of catalysts.

The chronoamperometric (CA) technique is an effective method to evaluate the electrocatalytic activity and stability of catalysts. Figure 5b shows current densities measured at 0.40 V for a period of 800 s in O_2-saturated 0.1 M $HClO_4$ solution. The high initial current was contributed to double layer charge and the large number of active Pt points on macroporous Pt electrode initially available for O_2 reduction. The prime current intensity on the macroporous Pt electrode was bigger than that on the Pd-modified macro-porous Pt electrode because there were more Pt active points on the macroporous Pt electrode than that on the Pd-modified macroporous Pt electrode. There are more active Pt points on the macroporous Pt electrode than that on the Pd-modified macroporous Pt because Pd modification makes active Pt point to decrease on the surface of the Pd modified Pt electrode. However, the stable current on Pd-modified macroporous electrode was bigger than that on the unmodified macroporous Pt electrode because unmodified macroporous Pt easily adsorbed OH than Pd-modified macroporous electrode. This confirms that Pd-modified macroporous Pt electrode has higher electrocatalytic activity than unmodified macro-porous Pt electrode for O_2 reduction.

3.5 Methanol oxidation on Pd-modified macroporous Pt electrode and macroporous Pt electrode

Cyclic voltammograms for the oxidation of methanol at Pd-modified macroporous Pt (solid line) and macroporous Pt (dashed line) are compared in Fig. 6. The forward scan is attributable to methanol oxidation, forming Pt-adsorbed carbonaceous intermediates. This adsorbed carbon monoxide (COads) causes the loss of activity of the electrocatalyst. [16] The backward oxidation peak is attributed to the additional oxidation of the adsorbed carbonaceous species to carbon dioxide [34, 35]. The maximum peak current for methanol oxidation at the macroporous Pt electrode was 6.0 mA cm^{-2}, which is three times of that (2.0 mA cm^{-2}) observed at the Pd-modified macroporous Pt electrode under identical working conditions. The electrocatalytic activity of macroporous Pt to methanol oxidation is much higher than that reported by Liu [36]. The high electrocatalytic activity of macroporous Pt for methanol oxidation may contribute to the macroporous structure of Pt electrode. Furthermore, the residual copper on macroporous Pt can enhance the electrocatalytic activity

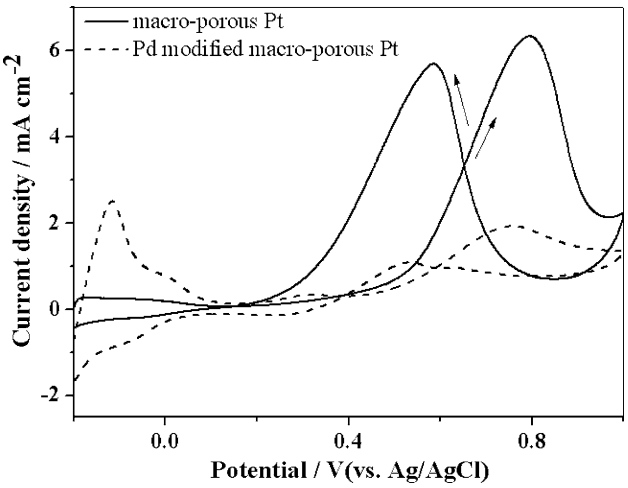

Fig. 6 CV imagine of Pd-modified macroporous Pt (*solid line*) and macroporous Pt (*dashed line*) in 0.1 M $HClO_4$ solution containing 1 M CH_3OH, scan rate 50 mV s^{-1}

to methanol oxidation [29]. According to bi-functional mechanism, the first step, the adsorption of CH_3OH on the surface, is in competition with the adsorption of spectator species, such as Hupd, OHads, and other species from the dissociation of the water and anions from the supported electrolyte. In the Fig. 6, a strong peak of Hupd can be observed on Pd-modified macroporous Pt electrode. It was found that CH_3OH can easily be displaced from the surface by these spectators; hence, in an electrochemical environment, the adsorption of CH_3OH molecules may occur only on bare metal sites. Therefore, these spectators in fact impede the electro-oxidation of methanol on the Pt surface. The Hupd is easily adsorbed on Pd-modified macroporous Pt electrode than on macroporous Pt electrode which can be clearly seen in Fig. 6. The high coverage of Hupd impedes the CH_3OH adsorbing on the electrode. Therefore, the current at Pd-modified macroporous Pt electrode was smaller than macroporous Pt electrode. In fact, methanol oxidation is highly inhibited on Pd modified macroporous Pt surfaces.

4 Conclusion

Macroporous Pt electrode was electrodeposited on PS by pulse deposition from the 0.1 M $HClO_4$ solution containing 0.2 mM H_2PtCl_6 and 1 mM copper ions. We presented here a novel electrochemical strategy to nanoparticle-based catalyst design using the UPD redox replacement technique. A single UPD Cu replacement with Pd^{2+} yielded an ultra thin and uniform Pd layer on macroporous Pt electrode. In this study, the electrocatalytic properties of Pd-modified macroporous Pt electrode and macro-porous Pt electrode investigated by cyclic voltammetry showed

that Pd-modified macroporous Pt electrode exhibited a higher catalytic activity to O_2 reduction than the macroporous Pt electrode, while the macroporous Pt electrode had high activity to methanol oxidation than Pd-modified macroporous Pt electrode.

Acknowledgment This study was supported by national science foundation of China (Grant No. 20775030).

References

1. Wang JX, Markovic NM, Adzic RR (2004) J Phys Chem B108:4127
2. Markovic NM, Ross PN (2000) Electrochim Acta 45:4101
3. Toda T, Igarashi H, Watanabe M (1999) J Electroanal Chem 460:258
4. Antolini E, Passos RR, Ticianelli EA (2002) Electrochim Acta 48:263
5. Kumar S, Zou SH (2006) Electrochem Comm 8:1151
6. Stamenkovic VR, Fowler B, Mum BS, Wang GF et al (2007) Science 315:493
7. Seminario M, Agapito LA, Yan L, Balbuena PB (2005) Chem Phy Let 410:275
8. Lee JK, Choi J, Kang SJ, Lee JM, Tak Y, Lee JY (2007) Electrochim Acta 52:2272
9. Valden M, Lai X, Goodman DW (1998) Science 281:1647
10. Rajesh B, Thampi KR, Bonard JM et al (2003) J Phys Chem B 107:2701
11. Salavagione HJ, Sanchis C, Morallon E (2007) J Phys Chem C 111:12454
12. Ye HC, Crooks RM (2005) J Am Chem Soc 127:4930
13. Attard GS, Bartlett PN, Coleman NRB, Elliott et al (1997) Science 278:838
14. Liu Y, Chen J, Misoska V, Swiegers GF et al (2007) Mater Lett 61:2887
15. Arico AS, Srinivasan S, Antonucci V (2001) Fuel Cells 1:133
16. Lin YH, Cui XL, Yen C, Wai CM (2005) J Phys Chem B 109:14410
17. Prabhuram J, Zhao TS, Tang ZK, Chen RZ et al (2006) J Phys Chem B 110:5245
18. Tsai MC, Yeh TK, Tsai CH (2006) Electrochem Comm 8:1445
19. Tremiliosi FG, Kim H, Chrzanowski W et al (1999) J Electroanal Chem 467:143
20. Christopher EL, Steven HB (1998) J Phys Chem B 102:193
21. Watanabe M, Motoo S (1975) J Electroanal Chem 60:267
22. Zhang J, Vukmirovic MB, Sasaki K (2005) J Am Chem Soc 127:12480
23. Kang S, Lee J, Lee JK, Chung SY, Tak Y (2006) J Phys Chem B 110:7270
24. Johnston CM, Strbac S, Lewera A, Sibert E et al (2006) Langmuir 22:8229
25. Eppler AS, Rupprechter G, Anderson EA et al (2000) J Phys Chem B 104:7286
26. Huang MH, Jin YD, Jiang HQ et al (2005) J Phys Chem B 109:15264
27. Holland BT, Blanford CF, Do T, Stein A (1999) Chem Mater 11:795
28. Jiang P, Bertone JF, Hwang KS, Colvin VL (1999) Chem Mater 11:2132
29. Du YL, Su BQ, Zhang N, Wang CM (2008) App Sur Sci 255:2641
30. Zhang J, Sasaki K, Sutter E, Adzic RR (2007) Science 315:220
31. Zhao MQ, Crooks RM (1999) Adv Mater 11:117
32. Vukmirovic MB, Zhang J, Sasaki K et al (2007) Electrochim Acta 52:2257
33. Liu H, Songa CJ, Zhang L, Zhang JJ et al (2006) J Power Sources 155:95
34. Yajima T, Uchida H, Watanabe M (2004) J Phys Chem B 108:2654
35. Huang JC, Liu ZL, He CB, Gan LM (2005) J Phys Chem B 109:16644
36. Liu F, Yan QF, Zhou WJ, Zhao XS, Lee JY (2006) Chem Mater 18:4328